Research Article

Intranasal vaccination induced cross-protective secretory IgA antibodies against SARS-CoV-2 variants with reducing the potential risk of lung eosinophilic immunopathology

Takuya Hemmi[1, 7], Akira Ainai[1, 7*], Takao Hashiguchi[2, 5], Minoru Tobiume[1], Takayuki Kanno[1], Naoko Iwata-Yoshikawa[1], Shun Iida[1], Yuko Sato[1], Sho Miyamoto[1], Akira Ueno[1, 6], Kaori Sano[1], Shinji Saito[1], Nozomi Shiwa-Sudo[1], Noriyo Nagata[1], Koji Tamura[7], Ryosuke Suzuki[3, 7], Hideki Hasegawa[4], Tadaki Suzuki[1]

[1] Department of Pathology, National Institute of Infectious Diseases.

[2] Laboratory of Medical Virology, Institute for Life and Medical Sciences, Kyoto University.

[3] Department of Virology II, National Institute of Infectious Diseases.

[4] Research Center for Influenza and Respiratory Virus, National Institute of Infectious

17 Diseases.

18 [5] Department of Virology, Faculty of Medicine, Kyushu University

19 [6] Department of Life Science and Medical Bioscience, Waseda University.

20 [7] Department of Biological Science and Technology, Tokyo University of Science.

21

22 * Correspondence to: Akira Ainai, PhD. Department of Pathology, National Institute of

23 Infectious Diseases, 1-23-1 Toyama, Shinjuku-ku, Tokyo, 162-8640 Japan. Tel:

24 +81-3-4582-2701; Fax: +81-3-5285-1189; E-mail: ainai@niid.go.jp

25

Abstract

To control the coronavirus disease 2019 (COVID-19) pandemic, there is a need to develop vaccines to prevent infection with severe acute respiratory syndrome coronavirus 2 (SARS-CoV-2) variants. One candidate is a nasal vaccine capable of inducing secretory IgA antibodies in the mucosa of the upper respiratory tract, the initial site of infection. However, regarding the development of COVID-19 vaccines, there is concern about the potential risk of inducing lung eosinophilic immunopathology as a vaccine-associated enhanced respiratory disease as a result of the T helper 2 (Th2)-dominant adaptive immune response. In this study, we investigated the protective effect against virus infection induced by intranasal vaccination of recombinant trimeric spike protein derived from SARS-CoV-2 adjuvanted with CpG oligonucleotides, ODN2006, in mouse model. The intranasal vaccine combined with ODN2006 successfully induced not only systemic spike-specific IgG antibodies, but also secretory IgA antibodies in the nasal mucosa. Secretory IgA antibodies showed high protective ability against SARS-CoV-2 variants (Alpha, Beta and Gamma variants) compared to IgG antibodies in the serum. The nasal vaccine of this formulation induced a high number of IFN-γ-secreting cells in the

42 draining cervical lymph nodes and a lower spike-specific IgG1/IgG2a ratio compared to
43 that of subcutaneous vaccination with alum as a typical Th2 adjuvant. These features are
44 consistent with the induction of the Th1 adaptive immune response. In addition, mice
45 intranasally vaccinated with ODN2006 showed less lung eosinophilic immunopathology
46 after viral challenge than mice subcutaneously vaccinated with alum adjuvant. Our
47 findings indicate that intranasal vaccine adjuvanted with ODN2006 could be a candidate
48 that can prevent the infection of antigenically different variant viruses, reducing the risk
49 of vaccine-associated enhanced respiratory disease.
50

51 **Keywords**: intranasal vaccination, secretory IgA antibody, COVID-19, SARS-CoV-2,
52 lung eosinophilic immunopathology
53

1. Introduction

The coronavirus disease 2019 (COVID-19) caused by severe acute respiratory syndrome coronavirus 2 (SARS-CoV-2) has spread worldwide since December 2019 and is presently a major public health concern [1, 2]. Vaccines could be the most promising approach to protect us from the threat of this infectious disease. In fact, several new vaccines have already been in use, showing high vaccine effectiveness [3-6]. Typical examples include the mRNA vaccines [3, 4] and the viral vector vaccines [5, 6]. Particularly in the UK, it is noteworthy that mRNA vaccine, BNT162b2 (Pfizer-BioNTech), was approved for practical use on December 2, 2020, less than a year after the epidemic began [7]. The advantage of the mRNA vaccine is that if the formulation of the vaccine has already been determined, a new vaccine can be launched for practical use in the shortest time, as long as the nucleic acid information of the target antigen is available. However, the long-term adverse events associated with the new modality of vaccines approved for emergency use are currently unknown; therefore, this issue should be adequately evaluated in the future. On the other hand, although the development of inactivated virus vaccines and subunit vaccines as conventional vaccine

70 formulations has been promoted, the development tends to be delayed because of time
71 taken to prepare the antigen. Unlike vaccines of new modality, these conventional
72 vaccines may have the advantage of being less burdensome to the vaccinees because
73 reactogenicity can be assumed to some extent.

74 Currently, most vaccines are administered intramuscularly or subcutaneously,
75 resulting in the induction of systemic antigen-specific IgG antibodies. In studies on nasal
76 influenza vaccines, we have already shown that a systemic antibody response is effective
77 for reducing mortality and morbidity associated with influenza but insufficient to prevent
78 infection, and that mucosal secretory IgA antibodies induced by intranasal vaccination
79 are highly protective against not only the vaccine-homologous virus but also
80 antigenically different viruses from the vaccine antigen [8-13]. The World Health
81 Organization (WHO) has recommended the development of a COVID-19 vaccine to
82 prevent infection with SARS-CoV-2 variants [14], therefore the study of vaccines
83 inducing mucosal immunity should be accelerated. In fact, 11 candidate intranasal
84 vaccines against SARS-CoV-2 have already been in clinical trials as of May 13, 2022 [15,
85 16].

However, there may be a risk of lung eosinophilic immunopathology caused by viral infection among COVID-19 vaccinators, a phenomenon known as vaccine-associated enhanced respiratory disease (VAERD) [17-23]. This phenomenon was first observed in the 1960s in a clinical trial of formalin-inactivated respiratory syncytial virus (FI-RSV) and measles vaccines. Two children died of severe pneumonia with eosinophilic infiltration due to natural infection after vaccination in the clinical trial of the FI-RSV vaccine [24]; thus, VAERD cannot be ignored in vaccine studies. Histological analysis of postmortem lung sections revealed immune complex formation and complement activation in the smaller airways. Similar eosinophilic immunopathology was observed in a mouse experiment with SARS-CoV and Middle East respiratory syndrome (MERS)-CoV vaccines. Some studies have suggested that lung eosinophilic immunopathology is due to the induction of T helper 2 (Th2)-shifted immune responses with high levels of antibody responses and insufficient neutralizing ability [21-23]. Although several studies on nasal COVID-19 vaccines in mouse models have already been reported, these studies did not analyze vaccine-induced eosinophilic immunopathology [25, 26]. Using a mouse model, we recently revealed that the

102 immunopathology of pneumonia with eosinophilic infiltration was induced by the
103 infection with SARS-CoV-2 among mice immunized with recombinant spike (S) protein
104 of the virus combined with alum adjuvant [23]. Thus, the U.S. Food and Drug
105 Administration (FDA) recommended that the balance of T-cell responses should be
106 properly assessed to avoid the risk of VAERD for vaccine candidates to be practically
107 used in the future[27].

108 In this study, we used a mouse model to evaluate both the protective effect and
109 neutralizing antibodies induced by intranasal administration of recombinant trimeric
110 spike protein derived from SARS-CoV-2 combined with synthetic oligodeoxynucleotides
111 containing the CpG motif, ODN2006 [28]. In addition, T-cell responses and the risk of
112 VAERD were examined after viral challenge in immunized mice. Our data showed that
113 intranasal administration of recombinant spike protein with ODN2006, rather than
114 subcutaneous administration in the presence of alum adjuvant, induced neutralizing
115 antibodies with well-balanced T-cell responses, resulting in the protection against
116 homologous or heterologous virus infection without lung eosinophilic immunopathology.
117

2. Materials and Methods

2.1. Purification of recombinant SARS-CoV-2 Spike protein

Recombinant trimeric ectodomain of SARS-CoV-2 S protein with two proline mutations (rtS-ecto2P) as a vaccine antigen was produced using a *Drosophila* expression system (Thermo Fisher Scientific, Grand Island, NY). The protein sequence was modified to remove the furin cleavage site (RRAR to GSAG), and two stabilizing mutations were introduced (K986P and V987P; wild-type numbering) [29, 30]. Protein expression and purification were performed as previously described [31]. Recombinant trimeric ectodomain of S protein with six proline mutations (rtS-ecto6P) for enzyme-linked immunosorbent assay (ELISA) was produced using Expi293F cells (Thermo Fisher Scientific). In addition to the mutation at the furin cleavage site, six stabilizing mutations were introduced (F817P, A892P, A899P, A942P, K986P, and V987P; wild-type numbering) [32].

2.2. Immunization and sampling

Female BALB/c mice (20-24 weeks old) (Japan SLC Inc., Hamamatsu, Shizuoka,

Japan) were maintained in specific pathogen-free facilities. The mice were either intranasally or subcutaneously vaccinated with 3 μg rtS-ecto2P three times at 2-week intervals. Intranasal vaccination was performed by instillation of 6 μL of vaccine solution with or without 10 μg of ODN2006 into each nostril (total, 12 μL/mouse). Subcutaneous vaccination was performed by inoculation with 100 μL of vaccine solution containing 10 μg of ODN2006 (InvivoGen, San Diego, CA) or 1 mg of Imject Alum adjuvant (Thermo Fisher Scientific) in the dorsal part of the cervical region. ODN2006 and Imject Alum were used as adjuvants to induce Th1- and Th2-dominant immune responses, respectively. For the time-course evaluation of the antibody response, partial blood sampling from the orbit was performed at 2-week intervals from the final vaccination. Serum, nasal and lung wash, and cervical lymph nodes were collected from mice for the evaluation of antibody and cellular immune responses, respectively, one week after the final vaccination.

All immunizations and partial blood sampling were performed under anesthesia. All animal experiments were performed in accordance with the Guide for Animal Experiments Performed at the National Institute of Infectious Diseases (NIID) and were approved by the Animal Care and Use Committee of NIID.

150

151 **2.3 Virus challenge and sampling**

152 To evaluate effectiveness of protection against virus infection, vaccinated mice were
153 inoculated intranasally with the mouse adapted SARS-CoV-2 strain, QHmusX (GenBank
154 Accession No.: LC605054) [23], into the lungs (40 LD_{50} per mouse) and nasal cavity (6
155 LD_{50} per mouse) 2 weeks after the final immunization. To protect against SARS-CoV-2
156 variants—Alpha variant QHN001 (lineage B.1.1.7, GISAID: EPI_ISL_804007), Beta
157 variant TY8-612 (lineage B.1.351, GISAID: EPI_ISL_1123289), and Gamma variant
158 TY7-501 (lineage P.1, GISAID: EPI_ISL_833366)—were intranasally challenged with
159 3.5×10^5 $TCID_{50}$ into the lungs and nasal cavity. Intranasal challenge into the upper and
160 lower respiratory tracts was performed by instillation of 30 µL and 4 µL (2 µL in each
161 nostril), respectively. To determine the viral titer in the nasal mucosa and lungs, nasal and
162 lung washes were collected 3 days after virus challenge, and the lungs were collected for
163 the evaluation of eosinophilic immunopathology at 6 days post-infection. In addition,
164 body weight was monitored for 10 days after the virus challenge. The humane endpoint
165 was defined as the appearance of clinical diagnostic signs of respiratory stress, including

166 respiratory distress and > 25% weight loss. The SARS-CoV-2 challenge was performed
167 in a biosafety level 3 facility according to the Guidelines for Animal Experiments
168 performed at NIID.
169
170 **2.4. Estimation of SARS-CoV-2 S-specific antibody responses**
171 SARS-CoV-2 S-specific antibodies were estimated using ELISA. Half-area
172 flat-bottomed microtiter plates (Corning Inc., NY) were coated with 50 ng/well
173 rtS-ecto6P, followed by blocking with PBS containing 5% skim milk and 0.05% Tween
174 20. Serial dilutions of serum samples from vaccinated mice were added to each well of
175 microtiter plates. IgG antibodies were detected using biotin-conjugated goat anti-mouse
176 IgG antibody (Jackson Immunoresearch, West Grove, PA), followed by alkaline
177 phosphatase-conjugated streptavidin (Invitrogen, CA, USA). The enzymatic reaction was
178 initiated by the addition of the substrate *p*-nitrophenylphosphate (Sigma-Aldrich,
179 Burlington, MA). The absorbance at 405 nm was measured using an iMark microplate
180 reader (Bio-Rad, Hercules, CA). All procedures were performed at room temperature.
181 The S-specific IgG antibody titer was defined as the reciprocal of the highest dilution of

182 the test sample, giving a higher absorbance than the cut-off value obtained as 2-fold mean
183 absorbance of serial dilutions of control naive mouse serum set in each plate.

184 Quantification of S-specific IgG1 or IgG2a antibodies in the serum and IgA
185 antibodies in nasal or lung washes was performed as previously described [23]. Chimeric
186 human-mouse monoclonal IgG1, IgG2a, and IgA antibodies bearing variable regions of
187 the S-specific human monoclonal antibody S309 [33] were used as standard antibodies
188 for quantification. Horseradish peroxidase (HRP)-conjugated polyclonal anti-mouse
189 IgG1 antibody (Bethyl Laboratories, Montgomery, TX), anti-mouse IgG2a antibody
190 (Bethyl Laboratories), or polyclonal anti-mouse IgA antibody (Bethyl Laboratories) were
191 used as detection antibodies. The enzymatic reaction was obtained by adding ABTS
192 substrate (Roche, Basel, Switzerland), and the absorbance of 405 nm was measured.

193

194 **2.5. SARS-CoV-2 neutralization assay**

195 The neutralization assay was performed as previously described [23, 34]. Briefly,
196 50uL of QHmusX (100TCID50) and 50uL of heat-inactivated serum serially diluted by
197 two-fold were mixed and incubated in 96-well microtiter plates for 1h at 37□, followed

198 by the addition of 100 μL of VeroE6-TMPRSS2 cells (JCRB1819, Japanese Collection of
199 Research Bioresources Cell Bank) [35, 36]. After five days of cultivation, samples were
200 examined for viral cytopathic effects (CPEs). Neutralizing antibody titers were
201 determined as the reciprocal of the highest dilution rate at which no CPEs were observed.
202 The neutralization assay was performed in a biosafety level 3 laboratory at the NIID,
203 Japan.
204
205 **2.6. Enzyme-linked immunospot assay**
206 Cells secreting interferon (IFN)-γ, interleukin (IL)-4, or IL-5 were determined using
207 a mouse enzyme-linked immunospot (ELISpot) assay kit (Mabtech, Cincinnati, OH)
208 according to the manufacturer's instructions. Briefly, in plates pre-coated with
209 anti-mouse IFN-γ, IL-4, or IL-5 antibodies, 3×10^5 cells harvested from the spleen or
210 cervical lymph nodes were incubated for 16 h in the presence of a peptide pool derived
211 from the S protein of SARS-CoV-2 (a mixture of PepTivator SARS-CoV-2 Prot_S, S1,
212 and S+; Miltenyi Biotec, Bergisch Gladbach, Germany). After washing the cells with
213 PBS, biotin-conjugated anti-IFN-γ, IL-4, or IL-5 detection antibodies were added and

214 incubated at RT for 2 h, followed by incubation with ALP-conjugated streptavidin at RT
215 for 1 h. The enzymatic reaction was initiated by addition of BCIP/NBT. Each experiment
216 was performed in duplicate. Spots formed by cytokine-secreting cells were counted and
217 analyzed using ELISpot reader S6 Universal with ImmunoSpot 7.0 software (Cellular
218 Technology, Ltd., Shaker Heights, OH).
219

220 **2.7. Flow cytometric analysis**

221 T follicular helper (Tfh) cells, germinal center B (GCB) cells, and eosinophils were
222 evaluated by flow cytometry. Single cell suspensions were obtained from the cervical
223 lymph nodes, spleen and lungs of immunized mice. One million cells were stained with
224 FVD506 (Thermo Fisher Scientific) for dead cell removal and blocked with anti-mouse
225 CD16/CD32 monoclonal antibody (BD Pharmingen, San Jose, CA). Cell surface markers
226 of Tfh cells were defined as $CD4^+$ $CD8^-$ $PD\text{-}1^+$ $CXCR5^+$ among $TER119^-$ Ly-6G/Ly-$6C^-$
227 $CD11b^-$ $CD19^-$ populations, and those of GCB cells were defined as $CD19^+$ $GL7^+$ $CD95^+$
228 cells among $TER119^-$ Ly-6G/Ly-$6C^-$ $CD11b^-$ $CD3^-$ populations [37]. Eosinophils are
229 defined as $CD45^+$ $CD11b^+$ $CD11c^-$ $Ly6G^+$ Siglec-F^- cells [38]. The antibodies used in

230 flow cytometric analysis are summarized in Supplementary Table 1. Samples were
231 analyzed with CantoII (BD Biosciences), and data were analyzed using FlowJo software
232 version 10.8.0 (Tree Star Inc., Ashland, OR).
233
234 **2.8. Quantification of SARS-CoV-2 subgenomic RNA**
235 Total RNA was extracted from 125 μL of nasal or lung wash using ISOGEN-LS
236 (Nippon gene, Toyko, Japan) and purified using a Maxwell RSC 48 Instrument (Promega,
237 Madison, WI) with a Maxwell RSC miRNA Plasma and Serum Kit (Promega).
238 Quantification of subgenomic RNA was performed by real-time reverse transcription
239 PCR (RT-PCR) using a QuantiTect Probe RT-PCR Kit (QIAGEN, Hilden, Germany) with
240 primers and probes as previously described [39]. Real-time RT-PCR was performed using
241 Mx3005P (Stratagene, La Jolla, CA, USA).
242
243 **2.9. Immunohistochemistry**
244 The lungs collected from mice were fixed in phosphate buffer containing 10% formalin.
245 The fixed lungs were embedded in paraffin and sectioned. Eosinophils were identified

using Astra Blue/Vital New Red staining (C.E.M. Stain Kit, Diagnostic Biosystems, Pleasanton, CA). The lung tissue sections were observed for eosinophil infiltration in the peribronchiolar areas using an optical microscope.

2.10. Statistical analysis

Data analysis and visualization were performed using GraphPad Prism 7.0 software (GraphPad Software Inc., San Diego, CA). For statistical analysis, the Kruskal-Wallis test with Dunn's multiple comparison test was used for comparisons between groups. Comparison of body weight and survival was performed using Dunnett's multiple comparisons test following the mixed-effects model or log-rank (Mantel-Cox) test, respectively. Statistical significance was set at $P < 0.05$.

3. Results

3.1. Intranasal vaccines induced S-specific antibodies in nasal mucosa and lung as well as serum

To evaluate the S-specific antibody responses, serum, nasal and lung wash

262 specimens were collected from mice that received three doses of either intranasal or
263 subcutaneous vaccines (Fig. 1A). Intranasal vaccination was performed with or without
264 ODN2006 as a mucosal adjuvant and subcutaneous vaccination was performed with
265 ODN2006 or alum adjuvant. Naïve mice were used as negative controls. Serum
266 S-specific IgG antibody titers and neutralization titers were determined using ELISA and
267 microneutralization assays, respectively. The concentration of S-specific IgA antibodies
268 in the nasal or lung wash samples was quantified using ELISA. Intranasal administration
269 without mucosal adjuvant induced low levels of serum S-specific IgG antibodies. In
270 contrast, intranasal vaccination adjuvanted with ODN2006 successfully induced
271 S-specific IgG antibodies in serum at a level similar to that induced by subcutaneous
272 vaccination in the presence of ODN2006 or alum adjuvant (Fig. 1B). The results for the
273 neutralizing antibody titer were similar to those of the S-specific IgG antibody titer (Fig.
274 1C). Although intranasal vaccination in the absence of mucosal adjuvant failed to induce
275 local antibody responses, nasal and lung S-specific IgA antibodies were detected among
276 intranasally immunized mice in the presence of ODN2006 (Fig. 1D and 1E). No secretory
277 IgA antibodies were detected in samples from subcutaneously vaccinated mice.

These results indicated that intranasal vaccination with ODN2006 as a mucosal adjuvant induced not only secretory IgA antibodies in the nasal mucosa and lungs but also systemic IgG antibodies at the same level as those obtained from subcutaneous vaccination with ODN2006 or alum adjuvant.

3.2. Intranasal vaccine adjuvanted with ODN2006 effectively protect mice from SARS-CoV-2 infection

To evaluate the protection against viral challenge, intranasal inoculation of the mouse-adapted SARS-CoV-2 strain, QHmusX, was performed on mice vaccinated under the same conditions as described above (Fig. 2A). Nasal and lung wash samples were collected at three days post-infection (dpi), and the amount of subgenomic RNA (sgRNA) derived from SARS-CoV-2 in these samples was evaluated by real-time RT-PCR to assess the protection of mice against infection. The number of sgRNA copies in the nasal wash was significantly reduced in mice with S-specific IgA in the nasal mucosa induced by intranasal vaccination adjuvanted with ODN2006 (Fig. 1D and 2B). No significant decrease in sgRNA in the nasal mucosa was observed in mice that received subcutaneous

294 vaccine or mice intranasally vaccinated with antigen only. A significant decrease in
295 sgRNA copies in the lung wash was observed in mice vaccinated intranasally or
296 subcutaneously in the presence of ODN2006 or alum, respectively, which showed high
297 neutralizing antibody titers in serum (Fig. 1C and 2C). Simultaneously, the mice were
298 monitored for body weight and survival for 10 days after the challenge (Fig. 2D and 2E).
299 Naïve mice and those intranasally vaccinated with antigen only died by 6 dpi. Among
300 mice that received subcutaneous vaccine with ODN2006 or alum, although few mice died,
301 others recovered from the apparent decrease in body weight post challenge and survived
302 until 10 dpi; in contrast, all mice intranasally vaccinated with ODN2006 survived without
303 remarkable body weight change during the observation period.

304 In addition, protection against viral challenge with SARS-CoV-2 variants (Alpha,
305 Beta and Gamma variants) was assessed (Fig. 3A). Significant reductions in nasal sgRNA
306 derived from each variant virus were achieved in mice intranasally vaccinated in the
307 presence of ODN2006 when compared to naïve mice (Fig. 3B-3D). In the lungs, sgRNA
308 of Alpha and Gamma variants significantly decreased by both intranasal and
309 subcutaneous vaccination with antigen together with ODN2006, while that of Beta

310 variant presented a significant decrease only by intranasal but not subcutaneous
311 vaccination (Fig. 3E-3G).

312 These findings indicate that IgA antibodies in the nasal mucosa and lung induced by
313 intranasal, but not subcutaneous, vaccination combined with ODN2006 were
314 cross-protective against SARS-CoV-2 variants.

315

316 **3.3. Formation of germinal center and maintenance of antibody responses by**
317 **intranasal vaccination**

318 The induction of memory B cells and long-lasting humoral immune responses
319 derived from long-lived plasma cells is important for successful vaccine-evoking
320 protective antibody responses [40]. The formation of a germinal center is required for the
321 affinity maturation of antibodies and determination of the B cell life span [37]. Hence,
322 vaccination-induced changes in the percentage of Tfh cells and GCB cells were evaluated
323 in lymphocytes from draining cervical lymph nodes using flow cytometry. The
324 proportions of both Tfh and GCB cells in cervical lymph nodes were definitely increased
325 by intranasal vaccination with antigen plus ODN2006 (Fig. 4A and 4B). In addition,

326 systemic S-specific IgG antibody responses were evaluated in serum samples collected
327 for 20 weeks at 2-week intervals after the initial vaccination (Fig. 4C). The highest
328 responses were achieved two weeks after the final vaccination, and mice that received
329 subcutaneous vaccine adjuvanted with alum or ODN2006 showed the highest S-specific
330 IgG antibodies, followed by mice intranasally vaccinated in the presence of ODN2006.
331 Although systemic S-specific IgG antibodies slightly declined over time during the
332 observation period, IgG antibodies were well held in mice subcutaneously vaccinated
333 with alum compared to mice that received intranasal or subcutaneous vaccination with
334 ODN2006 (Fig. 4D). At 20 weeks after the initial vaccination, S-specific nasal IgA
335 antibodies were detected in five out of six mice with intranasal vaccination combined
336 with ODN2006 but not in mice with other vaccinations (Fig. 4E).

337 Overall, these results suggest that intranasal vaccination with ODN2006 induced the
338 formation of GCs in the draining lymph nodes and the maintenance of local secretory IgA
339 antibody responses in the nasal mucosa, despite a slight decline in systemic IgG
340 responses.

341

3.4. Induction of Th1 response by using ODN2006 as an adjuvant

Lung eosinophilic immunopathology as a phenomenon of VAERD was observed in a clinical trial of FI-RSV and measles vaccine, and in a mouse model of SARS- or MERS-CoV vaccine. This phenomenon is suspected to be dependent on the Th2 dominant immune response of vaccine candidates [21-23]. Therefore, the Th response induced by intranasal vaccination with recombinant S protein in the presence of ODN2006 should be carefully examined. In mice, Th1 cells produce IFN-γ resulting in IgG2a induction, in contrast, Th2 cells produce IL-4 and IL-5 inducing IgG1 responses [41].

Cells isolated from the spleen and cervical lymph nodes one week after the final immunization were evaluated for cytokine production under stimulation of the peptide pool of S protein by ELISpot assay (Fig. 5A). Significant induction of IFN-γ-secreting cells was observed in the splenocytes of mice subcutaneously vaccinated with ODN2006 (Fig. 5B). In contrast, a significant induction of IL-4-secreting cells was observed in splenocytes obtained from mice subcutaneously vaccinated with alum adjuvant, and a similar tendency was observed in IL-5-secreting cells (Fig. 5C and 5D). In the case of

splenocytes, each cytokine-secreting cell significantly increased in mice that received subcutaneous vaccination with ODN2006 or alum but not in those intranasally vaccinated. Therefore, cytokine-secreting cells were evaluated using cells isolated from the draining cervical lymph nodes of intranasally vaccinated or naive mice. Intranasal vaccination in the presence of ODN2006 significantly increased the number of IFN-γ-secreting cells, while IL-4 and IL-5 secreting cells decreased compared to intranasal vaccines with only antigen (Fig. 5E). In contrast, intranasal vaccination with antigen in the absence of mucosal adjuvant significantly induced IL-4 and IL-5 secreting cells, but not IFN-γ-secreting cells, in draining lymph nodes (Fig 5F and 5G).

The dominant T cell response was estimated using an S-specific IgG antibody subclass (Fig. 5H and 5I). Large amounts of S-specific IgG1 antibodies were obtained in mice subcutaneously vaccinated with alum adjuvant compared to mice immunized in the presence of ODN2006; however, S-specific IgG2a antibodies in mice intranasally or subcutaneously vaccinated in the presence of ODN2006 were higher than those obtained in mice vaccinated with alum. When the S-specific IgG1/IgG2a ratio was calculated, the IgG1/IgG2a ratio after vaccination with ODN2006 was significantly lower than that after

vaccination with alum (Fig. 5J).

These results, obtained from the estimation of cytokine-secreting cells and IgG1/IgG2a ratio, suggested that ODN2006, used as an adjuvant, induced Th1 dominant immune responses regardless of the administration route.

3.5. Lung eosinophilic immunopathology is reduced by vaccines that induce a remarkable Th1 response

The correlation between vaccine-induced Th2 dominant immune responses and lung eosinophilic immunopathology was evaluated in a lethal challenge model in mice (Fig. 6A). S-specific IgG1/IgG2a ratios were calculated by ELISA in sera obtained one week prior to challenge, and eosinophilic infiltration into the lungs was examined at 6 dpi by histopathological and flow cytometric analyses. As shown in Fig. 6B, histological analysis revealed that mice immunized in the presence of ODN2006, regardless of the route of vaccination, showed small lesions with infiltration of inflammatory cells, including neutrophils and mononuclear cells around the blood vessels and bronchi, but little eosinophil infiltration. In contrast, eosinophilic infiltration around the bronchi and

390 blood vessels was observed in mice intranasally vaccinated with only antigen or
391 subcutaneously vaccinated with alum. Similar results were obtained in the flow
392 cytometric analysis. Although there were no significant differences in the percentages of
393 eosinophils induced among the different vaccines, these values correlated well with the
394 S-specific IgG1/IgG2a ratios ($r = 0.779$, $p = 0.0015$) (Fig. 6C and 6D).

395 Our results showed that Th2 dominant immune response, suspected by large values
396 of IgG1/IgG2a, caused lung eosinophilic immunopathology. In contrast, in immunization
397 combined with ODN2006, Th1 shifted immune responses correlating with low values of
398 IgG1/IgG2a ratio alleviated the risk of eosinophilic infiltration.

399

400 **4. Discussion**

401 In the current study, we revealed that intranasal vaccination with S protein together
402 with ODN2006, a toll-like receptor 9 agonist [28], could induce cross-protective
403 secretory IgA antibodies against SARS-CoV-2 variants in the nasal mucosa, which is the
404 initial site of infection. Furthermore, we demonstrated that this vaccine could reduce the
405 potential risk of lung eosinophilic immunopathology in the case of post-vaccination

406 infection.

407 In our previous studies on intranasal influenza vaccine, it has been revealed that
408 intranasal vaccination induces not only IgG antibodies in the serum but also
409 cross-protective secretory IgA antibodies on the surface of mucosal epithelial cells in the
410 upper respiratory tract [8-13]. Here, we evaluated serum and mucosal antibody responses
411 and protective effects induced in mice by intranasal vaccination with recombinant
412 SARS-CoV-2 S protein. Only mice immunized intranasally with antigen combined with
413 ODN2006 induced mucosal IgA as well as systemic IgG antibody responses
414 accompanied by a significant reduction in viral load in both the upper respiratory tract
415 and lungs. All individuals receiving this vaccine survived a lethal challenge with the
416 mouse adapted SARS-CoV-2 strain without significant weight loss. In addition, the
417 cross-protective ability by nasal vaccine was evaluated against SARS-CoV-2 Alpha, Beta
418 or Gamma variant. Results of neutralization assays using human sera collected from
419 mRNA vaccinees or individuals who suffered from breakthrough infections suggest that
420 the antigenicity of the Beta variant differs from those of the Alpha and Gamma variants.
421 [42-44]. When SARS-CoV-2 variants were challenged into the lungs, infections of Alpha

or Gamma variants were suppressed in mice intranasally or subcutaneously vaccinated, whereas infection with the Beta variant could not be prevented by either vaccination. On the other hand, all variants challenged into the nasal cavity were significantly prevented in mice possessing mucosal secretory IgA antibody induced by intranasal vaccination, but not in those subcutaneously vaccinated. These results indicate that, compared to systemic IgG antibodies which are primarily responsible for protection against infection in the lungs [11], secretory IgA antibodies that can be induced by intransal vaccination possess higher cross-protective activity against SARS-CoV-2 variantviruses with different antigenicities. Thus, a nasal vaccine that could induce highly cross-protective secretory IgA antibodies in the nasal mucosa, which is the gateway to respiratory infection, would be a more effective, reasonable vaccine candidate. It has been shown that the Omicron variant, which is currently prevalent around the world, could replicate more effectively in the bronchi than in the lungs, compared with other variants and the ancestor [45-48]. Therefore, there is high chance that a nasal vaccine which could induce cross-protective IgA antibodies in the upper respiratory tract would be effective against the Omicron variant as well.

When considering the COVID-19 vaccine, there is a concern about the potential risk of lung eosinophilic immunopathology in post-vaccination infections as VAERD. The FDA recommends addressing the potential risk of VAERD in animal models [27]. Since it has been considered that a Th2-dominant response increases the risk of VAERD, we investigated the T-cell response induced by intranasal vaccination combined with ODN2006 in detail. While IL-4- or IL-5-secreting cells were highly observed in spleen collected from mice subcutaneously vaccinated with alum as a typical Th2 adjuvant, individuals who received subcutaneous vaccination with ODN2006 showed high amounts of IFN-γ-secreting cells. Although nasal vaccination had no significant impact on spleen cells compared to subcutaneous vaccination, IFN-γ-secreting cells were significantly detected in draining cervical lymph nodes of intranasally vaccinated individuals with ODN2006. It was suggested that ELISpot assay using spleen cells might be unsuitable for the evaluation of T cell responses induced by intranasal vaccines. In contrast, the IgG1/IgG2a ratios determined from the quantification of S-specific IgG1 and IgG2 subclasses in serum were likely able to assess T cell responses reflecting neutralizing antibody titers, because the tendency to show similar levels of the

454 IgG1/IgG2a ratio among mice subcutaneously or intranasally vaccinated with ODN2006
455 was consistent with that of neutralizing antibody titers. Interestingly, eosinophil
456 infiltration into the lung correlated well with the serum IgG1/IgG2a ratio in our mouse
457 model. At this time, although the threshold for eosinophil infiltration that causes
458 eosinophilic pneumonia is unknown, analyzing immunization-induced IgG subclasses
459 could be an indicator for estimating whether there is a potential risk of VAERD. Although
460 several substances have been reported as potential mucosal adjuvants (e.g., cholera toxin
461 B subunit and synthetic double-stranded RNA), the potential risk of lung eosinophilic
462 immunopathology should be adequately investigated when designing a COVID-19
463 vaccine [8, 13].

464 In addition, the induction of B-cell memory and long-lived plasma cells by
465 vaccination is noteworthy, since germinal center formation is essential not only for the
466 production of high-affinity antibodies, but also for the determination of the B cell life
467 span.. The induction of Tfh and GCB cells by vaccination is essential to address this issue
468 [47, 49, 50]. In the current study, intranasal vaccination in the presence of ODN2006
469 successfully induced Tfh and GCB cells, long-lasting IgG antibodies in the serum, and

IgA antibodies in the nasal mucosa up to 16 weeks after the final vaccination.

Considering the emergence of new SARS-CoV-2 variants, nasal vaccines inducing a secretory IgA antibody with high cross-protective ability on the mucosal epithelium of the upper respiratory tract, which is the site of infection, could be highly useful, avoiding repeated vaccinations using newly manufactured antigens. In conclusion, our study showed that an intranasal COVID-19 vaccine of recombinant spike protein combined with an adjuvant inducing a Th1-shifted response would be a safe and effective vaccine not only for preparing cross-protective secretory IgA antibodies, but also to reduce the potential risk of VAERD, that is, lung eosinophilic immunopathology.

Acknowledgements

We thank A. Kojima and A. Sataka (Department of Pathology, NIID) and N. Kurisaki (Department of Virology, Kyushu Univ) for excellent support, and S. Takatsuka (Department of Fungal Infection, NIID) for technical suggestions and helpful discussions. Additionally, we would like to thank Editage (www.editage.com) for English language editing.

Author Contributions

Conceptualization: A.A, T.He., and T. S

Methodology: T.He., A.A., T.Ha., N.I.-Y., S.I., Y.S. A.U., K.S., N.S.-S., N.N. and T.S.

Investigation: T.He, T.Ha, M.T., T.K., N.I.-Y., Y.S., S.M., A.U., K.S., S.S. and A.A.

Visualization: T.He. and A.A.

Funding acquisition: H.H. and T.S.

Project administration: H.H. and T.S.

Supervision: R.S., K.T., H.H., and T.S.

Writing—Original draft: T.H. and A.A.

496 Writing—Review and editing: T.He., A.A., T.Ha., M.T., T.K., N.I.-Y., S.I., Y.S., S.M.,
497 A.U., K.S., S.S., N.S.-S., N.N., K.T., R.S., H.H. and T.S.

498

499 **Funding**

500 This work was supported in part by the Naito foundation, and by a Grant-in-Aid for
501 Research on Emerging and Reemerging Infectious Diseases from the Japanese Ministry
502 of Health, Labor and Welfare and the Japan Agency for Medical Research and
503 Development (AMED) under grant numbers JP20nk0101603, JP20nk0101604,
504 JP20nk0101626, JP20fk0108411 and JP21fk0108083. The funding agencies had no role
505 in the study design, data collection and analysis, decision to publish, or manuscript
506 preparation.

507

508 **Declaration of competing interest**

509 The authors declare that they have no known competing financial interests or personal
510 relationships that could have influenced the work reported in this study.

511

References

[1] Chen N, Zhou M, Dong X, Qu J, Gong F, Han Y, et al. Epidemiological and clinical characteristics of 99 cases of 2019 novel coronavirus pneumonia in Wuhan, China: a descriptive study. Lancet. 2020;395:507-13. https://doi.org/10.1016/S0140-6736(20)30211-7

[2] Zhu N, Zhang D, Wang W, Li X, Yang B, Song J, et al. A Novel Coronavirus from Patients with Pneumonia in China, 2019. N Engl J Med. 2020;382:727-33. https://doi.org/10.1056/NEJMoa2001017

[3] Polack FP, Thomas SJ, Kitchin N, Absalon J, Gurtman A, Lockhart S, et al. Safety and Efficacy of the BNT162b2 mRNA Covid-19 Vaccine. N Engl J Med. 2020;383:2603-15. https://doi.org/10.1056/NEJMoa2034577

[4] Baden LR, El Sahly HM, Essink B, Kotloff K, Frey S, Novak R, et al. Efficacy and Safety of the mRNA-1273 SARS-CoV-2 Vaccine. N Engl J Med. 2021;384:403-16. https://doi.org/10.1056/NEJMoa2035389

[5] Knoll MD, Wonodi C. Oxford-AstraZeneca COVID-19 vaccine efficacy. Lancet. 2021;397:72-4. https://doi.org/10.1016/S0140-6736(20)32623-4

528 [6] Sadoff J, Gray G, Vandebosch A, Cardenas V, Shukarev G, Grinsztejn B, et al.
529 Safety and Efficacy of Single-Dose Ad26.COV2.S Vaccine against Covid-19. N Engl J
530 Med. 2021;384:2187-201. https://doi.org/10.1056/NEJMoa2101544
531 [7] Medicines and Healthcare products Regulatory Agency. UK medicines regulator
532 gives approval for first UK COVID-19 vaccine.,
533 https://www.gov.uk/government/news/uk-medicines-regulator-gives-approval-for-first-u
534 k-covid-19-vaccine; 2020 [accessed 15 May 2022]
535 [8] Tamura S, Samegai Y, Kurata H, Nagamine T, Aizawa C, Kurata T. Protection
536 against influenza virus infection by vaccine inoculated intranasally with cholera toxin B
537 subunit. Vaccine. 1988;6:409-13. https://doi.org/10.1016/0264-410x(88)90140-5
538 [9] Tamura S, Funato H, Hirabayashi Y, Kikuta K, Suzuki Y, Nagamine T, et al.
539 Functional role of respiratory tract haemagglutinin-specific IgA antibodies in protection
540 against influenza. Vaccine. 1990;8:479-85.
541 https://doi.org/10.1016/0264-410x(90)90250-p
542 [10] Tamura S, Funato H, Hirabayashi Y, Suzuki Y, Nagamine T, Aizawa C, et al.
543 Cross-protection against influenza A virus infection by passively transferred respiratory

544 tract IgA antibodies to different hemagglutinin molecules. Eur J Immunol.
545 1991;21:1337-44. https://doi.org/10.1002/eji.1830210602

546 [11] Asahi Y, Yoshikawa T, Watanabe I, Iwasaki T, Hasegawa H, Sato Y, et al.
547 Protection against influenza virus infection in polymeric Ig receptor knockout mice
548 immunized intranasally with adjuvant-combined vaccines. J Immunol. 2002;168:2930-8.
549 https://doi.org/10.4049/jimmunol.168.6.2930

550 [12] Asahi-Ozaki Y, Yoshikawa T, Iwakura Y, Suzuki Y, Tamura S, Kurata T, et al.
551 Secretory IgA antibodies provide cross-protection against infection with different strains
552 of influenza B virus. J Med Virol. 2004;74:328-35. https://doi.org/10.1002/jmv.20173

553 [13] Ichinohe T, Watanabe I, Ito S, Fujii H, Moriyama M, Tamura S, et al. Synthetic
554 double-stranded RNA poly(I:C) combined with mucosal vaccine protects against
555 influenza virus infection. J Virol. 2005;79:2910-9.
556 https://doi.org/10.1128/JVI.79.5.2910-2919.2005

557 [14] World Health Organization. Interim Statement on COVID-19 vaccines in the
558 context of the circulation of the Omicron SARS-CoV-2 Variant from the WHO
559 Technical Advisory Group on COVID-19 Vaccine Composition (TAG-CO-VAC),

https://www.who.int/news/item/11-01-2022-interim-statement-on-covid-19-vaccines-in-the-context-of-the-circulation-of-the-omicron-sars-cov-2-variant-from-the-who-technical-advisory-group-on-covid-19-vaccine-composition; 2022 [accessed 6 May 2022]

[15] World Health Organization. The COVID-19 vaccine tracker and landscape compiles detailed information of each COVID-19 vaccine candidate in development by closely monitoring their progress through the pipeline., https://www.who.int/publications/m/item/draft-landscape-of-covid-19-candidate-vaccines; 2022 [accessed 6 May 2022]

[16] Alu A, Chen L, Lei H, Wei Y, Tian X, Wei X. Intranasal COVID-19 vaccines: From bench to bed. EBioMedicine. 2022;76:103841. https://doi.org/10.1016/j.ebiom.2022.103841

[17] Bolles M, Deming D, Long K, Agnihothram S, Whitmore A, Ferris M, et al. A double-inactivated severe acute respiratory syndrome coronavirus vaccine provides incomplete protection in mice and induces increased eosinophilic proinflammatory pulmonary response upon challenge. J Virol. 2011;85:12201-15. https://doi.org/10.1128/JVI.06048-11

576 [18] Tseng CT, Sbrana E, Iwata-Yoshikawa N, Newman PC, Garron T, Atmar RL, et al.
577 Immunization with SARS coronavirus vaccines leads to pulmonary immunopathology
578 on challenge with the SARS virus. PLoS One. 2012;7:e35421.
579 https://doi.org/10.1371/journal.pone.0035421
580 [19] Yasui F, Kai C, Kitabatake M, Inoue S, Yoneda M, Yokochi S, et al. Prior
581 immunization with severe acute respiratory syndrome (SARS)-associated coronavirus
582 (SARS-CoV) nucleocapsid protein causes severe pneumonia in mice infected with
583 SARS-CoV. J Immunol. 2008;181:6337-48.
584 https://doi.org/10.4049/jimmunol.181.9.6337
585 [20] Sekimukai H, Iwata-Yoshikawa N, Fukushi S, Tani H, Kataoka M, Suzuki T, et al.
586 Gold nanoparticle-adjuvanted S protein induces a strong antigen-specific IgG response
587 against severe acute respiratory syndrome-related coronavirus infection, but fails to
588 induce protective antibodies and limit eosinophilic infiltration in lungs. Microbiol
589 Immunol. 2020;64:33-51. https://doi.org/10.1111/1348-0421.12754
590 [21] Iwata-Yoshikawa N, Uda A, Suzuki T, Tsunetsugu-Yokota Y, Sato Y, Morikawa S,
591 et al. Effects of Toll-like receptor stimulation on eosinophilic infiltration in lungs of

592 BALB/c mice immunized with UV-inactivated severe acute respiratory
593 syndrome-related coronavirus vaccine. J Virol. 2014;88:8597-614.
594 https://doi.org/10.1128/JVI.00983-14
595 [22] Honda-Okubo Y, Barnard D, Ong CH, Peng BH, Tseng CT, Petrovsky N. Severe
596 acute respiratory syndrome-associated coronavirus vaccines formulated with delta
597 inulin adjuvants provide enhanced protection while ameliorating lung eosinophilic
598 immunopathology. J Virol. 2015;89:2995-3007. https://doi.org/10.1128/JVI.02980-14
599 [23] Iwata-Yoshikawa N, Shiwa N, Sekizuka T, Sano K, Ainai A, Hemmi T, et al. A
600 lethal mouse model for evaluating vaccine-associated enhanced respiratory disease
601 during SARS-CoV-2 infection. Sci Adv. 2022;8:eabh3827.
602 https://doi.org/10.1126/sciadv.abh3827
603 [24] Kim HW, Canchola JG, Brandt CD, Pyles G, Chanock RM, Jensen K, et al.
604 Respiratory syncytial virus disease in infants despite prior administration of antigenic
605 inactivated vaccine. Am J Epidemiol. 1969;89:422-34.
606 https://doi.org/10.1093/oxfordjournals.aje.a120955
607 [25] An X, Martinez-Paniagua M, Rezvan A, Sefat SR, Fathi M, Singh S, et al.

608 Single-dose intranasal vaccination elicits systemic and mucosal immunity against
609 SARS-CoV-2. iScience. 2021;24:103037. https://doi.org/10.1016/j.isci.2021.103037
610 [26] Du Y, Xu Y, Feng J, Hu L, Zhang Y, Zhang B, et al. Intranasal administration of a
611 recombinant RBD vaccine induced protective immunity against SARS-CoV-2 in mouse.
612 Vaccine. 2021;39:2280-7. https://doi.org/10.1016/j.vaccine.2021.03.006
613 [27] U.S. Food and Drug Administration. Development and licensure of vaccines to
614 prevent COVID-19,
615 https://www.fda.gov/regulatory-information/search-fda-guidance-documents/developme
616 nt-and-licensure-vaccines-prevent-covid-19; 2020 [accessed 6 May 2022]
617 [28] Nakagawa T, Tanino T, Onishi M, Tofukuji S, Kanazawa T, Ishioka Y, et al.
618 S-540956, a CpG Oligonucleotide Annealed to a Complementary Strand With an
619 Amphiphilic Chain Unit, Acts as a Potent Cancer Vaccine Adjuvant by Targeting
620 Draining Lymph Nodes. Front Immunol. 2021;12:803090.
621 https://doi.org/10.3389/fimmu.2021.803090
622 [29] Amanat F, Stadlbauer D, Strohmeier S, Nguyen THO, Chromikova V, McMahon M,
623 et al. A serological assay to detect SARS-CoV-2 seroconversion in humans. Nat Med.

624 2020;26:1033-6. https://doi.org/10.1038/s41591-020-0913-5

625 [30] Onodera T, Kita S, Adachi Y, Moriyama S, Sato A, Nomura T, et al. A

626 SARS-CoV-2 antibody broadly neutralizes SARS-related coronaviruses and variants by

627 coordinated recognition of a virus-vulnerable site. Immunity. 2021;54:2385-98 e10.

628 https://doi.org/10.1016/j.immuni.2021.08.025

629 [31] Hashiguchi T, Fukuda Y, Matsuoka R, Kuroda D, Kubota M, Shirogane Y, et al.

630 Structures of the prefusion form of measles virus fusion protein in complex with

631 inhibitors. Proc Natl Acad Sci U S A. 2018;115:2496-501.

632 https://doi.org/10.1073/pnas.1718957115

633 [32] Hsieh CL, Goldsmith JA, Schaub JM, DiVenere AM, Kuo HC, Javanmardi K, et al.

634 Structure-based design of prefusion-stabilized SARS-CoV-2 spikes. Science.

635 2020;369:1501-5. https://doi.org/10.1126/science.abd0826

636 [33] Pinto D, Park YJ, Beltramello M, Walls AC, Tortorici MA, Bianchi S, et al.

637 Cross-neutralization of SARS-CoV-2 by a human monoclonal SARS-CoV antibody.

638 Nature. 2020;583:290-5. https://doi.org/10.1038/s41586-020-2349-y

639 [34] Moriyama S, Adachi Y, Sato T, Tonouchi K, Sun L, Fukushi S, et al. Temporal

640 maturation of neutralizing antibodies in COVID-19 convalescent individuals improves
641 potency and breadth to circulating SARS-CoV-2 variants. Immunity. 2021;54:1841-52
642 e4. https://doi.org/10.1016/j.immuni.2021.06.015
643 [35] Nao N, Sato K, Yamagishi J, Tahara M, Nakatsu Y, Seki F, et al. Consensus and
644 variations in cell line specificity among human metapneumovirus strains. PLoS One.
645 2019;14:e0215822. https://doi.org/10.1371/journal.pone.0215822
646 [36] Matsuyama S, Nao N, Shirato K, Kawase M, Saito S, Takayama I, et al. Enhanced
647 isolation of SARS-CoV-2 by TMPRSS2-expressing cells. Proc Natl Acad Sci U S A.
648 2020;117:7001-3. https://doi.org/10.1073/pnas.2002589117
649 [37] Tian JH, Patel N, Haupt R, Zhou H, Weston S, Hammond H, et al. SARS-CoV-2
650 spike glycoprotein vaccine candidate NVX-CoV2373 immunogenicity in baboons and
651 protection in mice. Nat Commun. 2021;12:372.
652 https://doi.org/10.1038/s41467-020-20653-8
653 [38] Misharin AV, Morales-Nebreda L, Mutlu GM, Budinger GR, Perlman H. Flow
654 cytometric analysis of macrophages and dendritic cell subsets in the mouse lung. Am J
655 Respir Cell Mol Biol. 2013;49:503-10. https://doi.org/10.1165/rcmb.2013-0086MA

656 [39] Ishii H, Nomura T, Yamamoto H, Nishizawa M, Thu Hau TT, Harada S, et al.
657 Neutralizing-antibody-independent SARS-CoV-2 control correlated with
658 intranasal-vaccine-induced CD8(+) T cell responses. Cell Rep Med. 2022;3:100520.
659 https://doi.org/10.1016/j.xcrm.2022.100520
660 [40] Hassan AO, Shrihari S, Gorman MJ, Ying B, Yaun D, Raju S, et al. An intranasal
661 vaccine durably protects against SARS-CoV-2 variants in mice. Cell Rep.
662 2021;36:109452. https://doi.org/10.1016/j.celrep.2021.109452
663 [41] Toellner KM, Luther SA, Sze DM, Choy RK, Taylor DR, MacLennan IC, et al. T
664 helper 1 (Th1) and Th2 characteristics start to develop during T cell priming and are
665 associated with an immediate ability to induce immunoglobulin class switching. J Exp
666 Med. 1998;187:1193-204. https://doi.org/10.1084/jem.187.8.1193
667 [42] Kotaki R, Adachi Y, Moriyama S, Onodera T, Fukushi S, Nagakura T, et al.
668 SARS-CoV-2 Omicron-neutralizing memory B cells are elicited by two doses of
669 BNT162b2 mRNA vaccine. Sci Immunol. 2022;7:eabn8590.
670 https://doi.org/10.1126/sciimmunol.abn8590
671 [43] Mantus G, Nyhoff LE, Edara VV, Zarnitsyna VI, Ciric CR, Flowers MW, et al.

672 Pre-existing SARS-CoV-2 immunity influences potency, breadth, and durability of the
673 humoral response to SARS-CoV-2 vaccination. Cell Rep Med. 2022;3:100603.
674 https://doi.org/10.1016/j.xcrm.2022.100603
675 [44] Miyamoto S, Arashiro T, Adachi Y, Moriyama S, Kinoshita H, Kanno T, et al.
676 Vaccination-infection interval determines cross-neutralization potency to SARS-CoV-2
677 Omicron after breakthrough infection by other variants. Med (NY). 2022;3:249-61 e4.
678 https://doi.org/10.1016/j.medj.2022.02.006
679 [45] Halfmann PJ, Iida S, Iwatsuki-Horimoto K, Maemura T, Kiso M, Scheaffer SM, et
680 al. SARS-CoV-2 Omicron virus causes attenuated disease in mice and hamsters. Nature.
681 2022;603:687-92. https://doi.org/10.1038/s41586-022-04441-6
682 [46] Hui KPY, Ho JCW, Cheung MC, Ng KC, Ching RHH, Lai KL, et al. SARS-CoV-2
683 Omicron variant replication in human bronchus and lung ex vivo. Nature.
684 2022;603:715-20. https://doi.org/10.1038/s41586-022-04479-6
685 [47] Haque A, Pant AB. Mitigating Covid-19 in the face of emerging virus variants,
686 breakthrough infections and vaccine hesitancy. J Autoimmun. 2022;127:102792.
687 https://doi.org/10.1016/j.jaut.2021.102792

688 [48] Uraki R, Kiso M, Iida S, Imai M, Takashita E, Kuroda M, et al. Characterization
689 and antiviral susceptibility of SARS-CoV-2 Omicron/BA.2. Nature. 2022.
690 https://doi.org/10.1038/s41586-022-04856-1
691 [49] Crotty S. T follicular helper cell differentiation, function, and roles in disease.
692 Immunity. 2014;41:529-42. https://doi.org/10.1016/j.immuni.2014.10.004
693 [50] Quast I, Tarlinton D. B cell memory: understanding COVID-19. Immunity.
694 2021;54:205-10. https://doi.org/10.1016/j.immuni.2021.01.014
695
696

697 **Figure legends**

698

699 **Fig. 1. The induction of S-specific antibodies in serum, nasal mucosa and lungs of**
700 **mice vaccinated intranasally.**

701 (**A**) Each of six mice were vaccinated three times at 2-week intervals. One week after the
702 final vaccination, serum, nasal wash (NW) and lung wash (LW) were collected for the
703 evaluation of antibody responses. (**B**, **C**) SARS-CoV-2 S-specific IgG titers and
704 neutralizing antibody titers in sera were measured by ELISA and microneutralization
705 assay, respectively. Graphs shown as the geometric mean titers ± the geometric standard
706 deviation (SD). The dashed line indicates the detection limit of measurement. (**D**, **E**) The
707 concentration of S-specific IgA antibodies in NW and LW was estimated by ELISA. Data
708 shown as the means ± SD. Each dotted line indicates the detection limit of measurement.
709 The p-values were calculated by Kruskal-Wallis test followed by Dunn's multiple
710 comparison test (*P < 0.05, **P < 0.01). in: intranasally, sc: subcutaneously.

711

712 **Fig. 2. Intranasal vaccination adjuvanted with ODN2006 protected mice from the**

713 **lethal challenge with SARS-CoV-2.**

714 (**A**) Each of 12 mice were vaccinated three times at 2-week intervals. Two weeks after the
715 final vaccination, mice were intranasally challenged with mouse adopted SARS-CoV-2
716 strain, QHmusX, into both lungs and nasal cavity (40 and 6 LD_{50} per mouse, respectively).
717 NW and LW were collected from each of six mice for the evaluation of antibody
718 responses at 3 dpi. Body weight and survival of six mice were monitored 10 days after
719 viral challenge. (**B**, **C**) Copy numbers of SARS-CoV-2 subgenomic RNA (sgRNA) in
720 NW and LW were evaluated by real-time RT-PCR. Data shown as the geometric mean ±
721 the geometric SD. The p-values were calculated by Kruskal-Wallis test followed by
722 Dunn's multiple comparison test (*P < 0.05, *** P < 0.001). (**D**, **E**) Body weight changes
723 and survival rates during 10 days of observation after challenge with QHmusX. Data
724 shown as the means ± SD. The p-values of body weight and survival were compared with
725 mice intranasally vaccinated with ODN2006 by mixed-model analysis followed by
726 Dunnett's multiple comparisons test and log-rank (Mantel-Cox) test (**P < 0.01).

727

728 **Fig. 3. Secretory IgA antibodies were protective against SARS-CoV-2 variants.**

(**A**) Mice were vaccinated three times at 2-week intervals. Two weeks after the final vaccination, each of six mice were intranasally challenged with 3.5×10^5 $TCID_{50}$ of Alpha (**B**, **E**), Beta (**C**, **F**) or Gamma (**D**, **G**) variant into both lungs and nasal cavity. At 3 dpi, NW and LW were collected. Copy numbers of sgRNA in NW (**B**-**D**) and LW (**E**-**G**) were evaluated by real-time RT-PCR. Data shown as the geometric mean ± the geometric SD. The p-values were calculated by Kruskal-Wallis test followed by Dunn's multiple comparison test (*P < 0.05, *** P < 0.001).

Fig. 4. Germinal center formation and long-lasting antibody responses.

(**A**, **B**) The frequency of Tfh cells ($CXCR5^+$ $PD\text{-}1^+$) among $CD4^+$ cells and GCB cells ($GL7^+$ $CD95^+$) among $CD19^+$ B cells was evaluated by flow cytometry in cervical lymph nodes collected from mice one week after third vaccination. Results were shown as the mean ± SD. (**C**) To evaluate time-course of antibody responses induced by three doses of vaccination, serum samples were collected every two weeks. After 20 weeks from the initial vaccination, serum and NW samples were collected (six mice per group). (**D**) The changes of optical density (405 nm) of S-specific IgG antibodies were shown as the mean

± SEM. (**E**) S-specific IgA concentration in NW collected at 20 weeks after the initial vaccination was evaluated by ELISA. Results were shown as the mean ± SD. Each dotted line indicates the detection limit of measurement. The p-values were calculated by Kruskal-Wallis test followed by Dunn's multiple comparison test (*P < 0.05, **P < 0.01, ***P < 0.001).

Fig. 5. Induction of significant Th1 response by using ODN2006 as an adjuvant.

(**A**) Spleen and cervical lymph nodes were collected from individuals shown in Figure.1(**A**). Single cell suspensions obtained from each tissue was cultured under the stimulation of peptide pool of SARS-CoV-2 S protein. Spleen (**B**-**D**) or cervical lymph node cells (**E**-**G**) were counted on the production of IFN-r (**B**, **E**), IL-4 (**C**, **F**) and IL-5 (**D**, **G**) by ELISpot assay. Data shown as the means ± SD. (**H**, **I**) SARS-CoV-2 S-specific IgG1 and IgG2a antibodies were quantified by ELISA, and (**J**) IgG1/IgG2a ratio was calculated. Data shown as the geometric means ± geometric SD. The p-values were calculated by Kruskal-Wallis test followed by Dunn's multiple comparison test (*P < 0.05, **P < 0.01, ***P < 0.001).

Fig. 6. Eosinophilic infiltration into the lungs was suppressed in mice vaccinated with ODN2006 inducing a remarkable Th1 response.

(**A**) Each of six mice were vaccinated three times at 2-week intervals. Two weeks after the final vaccination, mice were intranasally challenged with mouse adopted SARS-CoV-2 strain, QHmusX, into both lungs and nasal cavity (40 LD_{50} and 6 LD_{50} per mouse, respectively). At 6 dpi, infiltration of eosinophils was evaluated by histopathological or flow cytometric analysis, on lungs collected from surviving 1~2 or 2~4 mice in each group, respectively. (**B**) Histopathological findings of mouse lungs by eosinophil staining using the combined eosinophil-mast cell staining (C.E.M.) kit. Green arrow heads point to eosinophils. The images in the lower panels are enlargements of area boxed in the upper images. The scale bar is 200 μm for low magnification and 20 μm for high magnification. (**C**) The percentage of eosinophils ($CD11b^+$ $CD11c^-$ $Siglec\text{-}F^+$ $Ly\text{-}6G^-$) among CD45+ cells was analyzed by flow cytometry. Results were shown as the mean ± SD. The p-values were calculated by Kruskal-Wallis test followed by Dunn's multiple comparison test. (**D**) Correlation between S-specific IgG1/IgG2a ratio and the frequency

777 of eosinophils in lung cells was analyzed by Spearman correlation. S-specific

778 IgG1/IgG2a ratio was evaluated using serum samples collected seven days before the

779 virus challenge.

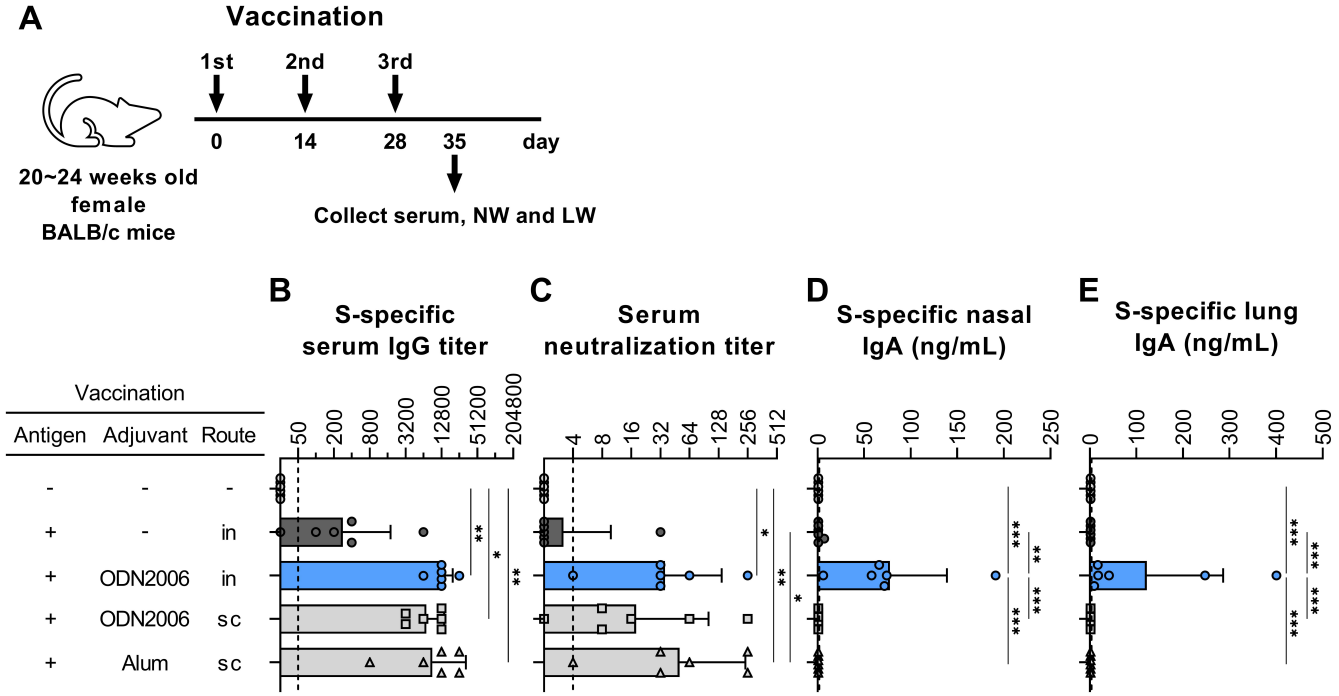
A
Vaccination
1st
2nd
3rd
0
14
28
35
day
20~24 weeks old
female
BALB/c mice
Collect serum, NW and LW
B
S-specific
serum IgG titer
C
Serum
neutralization titer
D
S-specific nasal
IgA (ng/mL)
E
S-specific lung
IgA (ng/mL)
Vaccination
Antigen
Adjuvant
Route
-
-
-
+
-
in
+
ODN2006
in
+
ODN2006
sc
+
Alum
sc
50
200
800
3200
12800
51200
204800
4
8
16
32
64
128
256
512
0
50
100
150
200
250
0
100
200
300
400
500
*
**
***

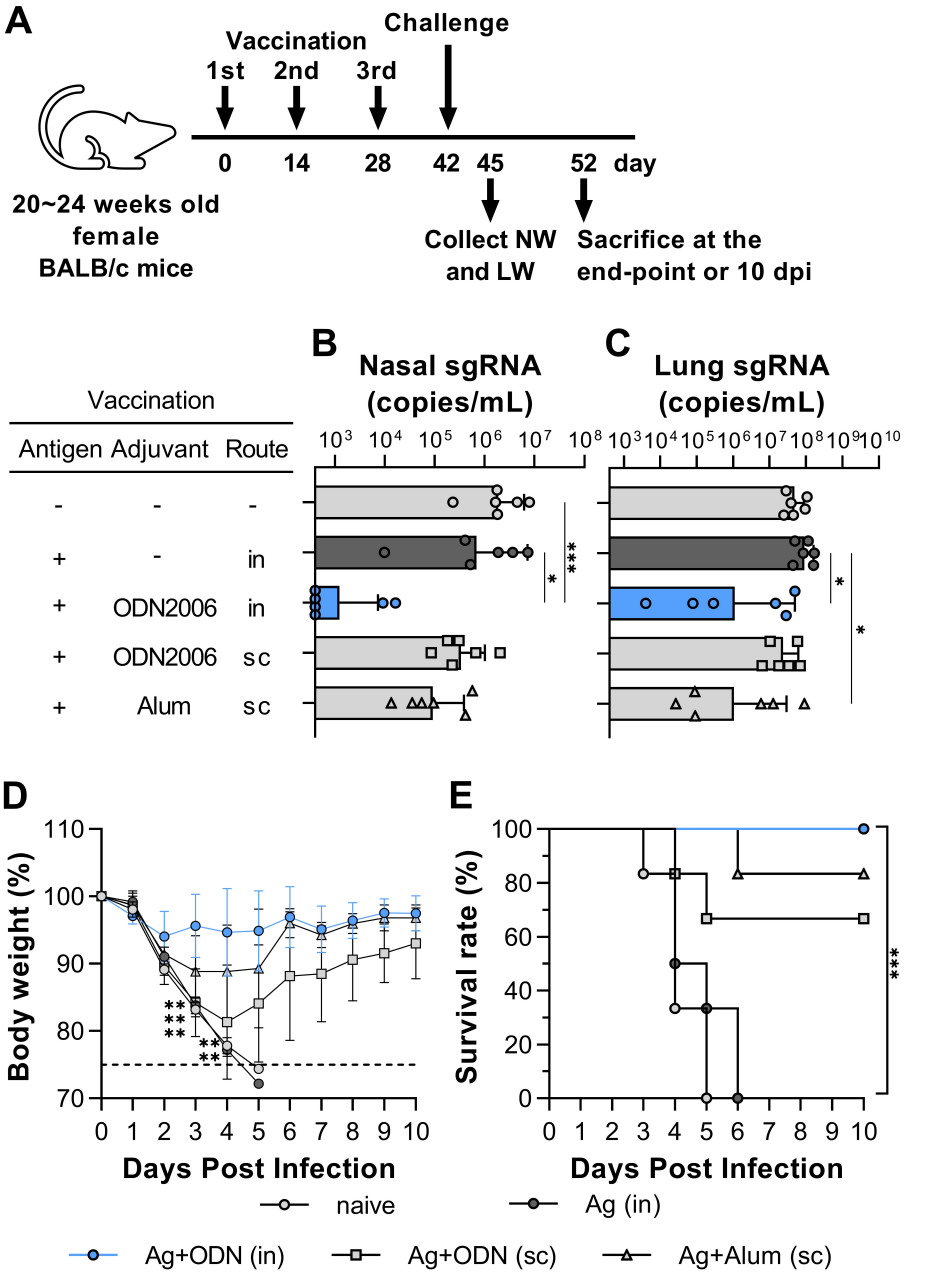
A
Vaccination
1st
2nd
3rd
Challenge
0
14
28
42
45
52
day
20~24 weeks old female BALB/c mice
Collect NW and LW
Sacrifice at the end-point or 10 dpi
Vaccination
Antigen Adjuvant Route
- - -
+ - in
+ ODN2006 in
+ ODN2006 sc
+ Alum sc
B
Nasal sgRNA (copies/mL)
C
Lung sgRNA (copies/mL)
D
Body weight (%)
Days Post Infection
E
Survival rate (%)
Days Post Infection
naive
Ag (in)
Ag+ODN (in)
Ag+ODN (sc)
Ag+Alum (sc)

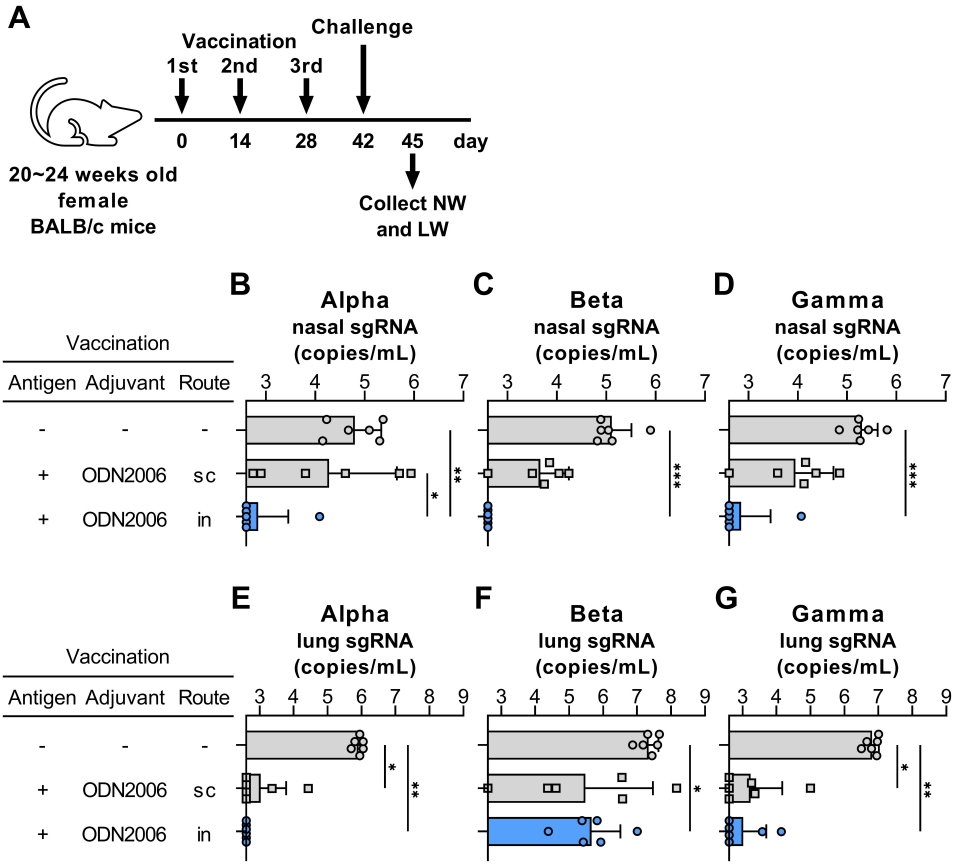
A
Vaccination
1st
2nd
3rd
Challenge
0
14
28
42
45
day
20~24 weeks old
female
BALB/c mice
Collect NW
and LW
B
Alpha
nasal sgRNA
(copies/mL)
C
Beta
nasal sgRNA
(copies/mL)
D
Gamma
nasal sgRNA
(copies/mL)
Vaccination
Antigen Adjuvant Route
- - -
+ ODN2006 sc
+ ODN2006 in
E
Alpha
lung sgRNA
(copies/mL)
F
Beta
lung sgRNA
(copies/mL)
G
Gamma
lung sgRNA
(copies/mL)

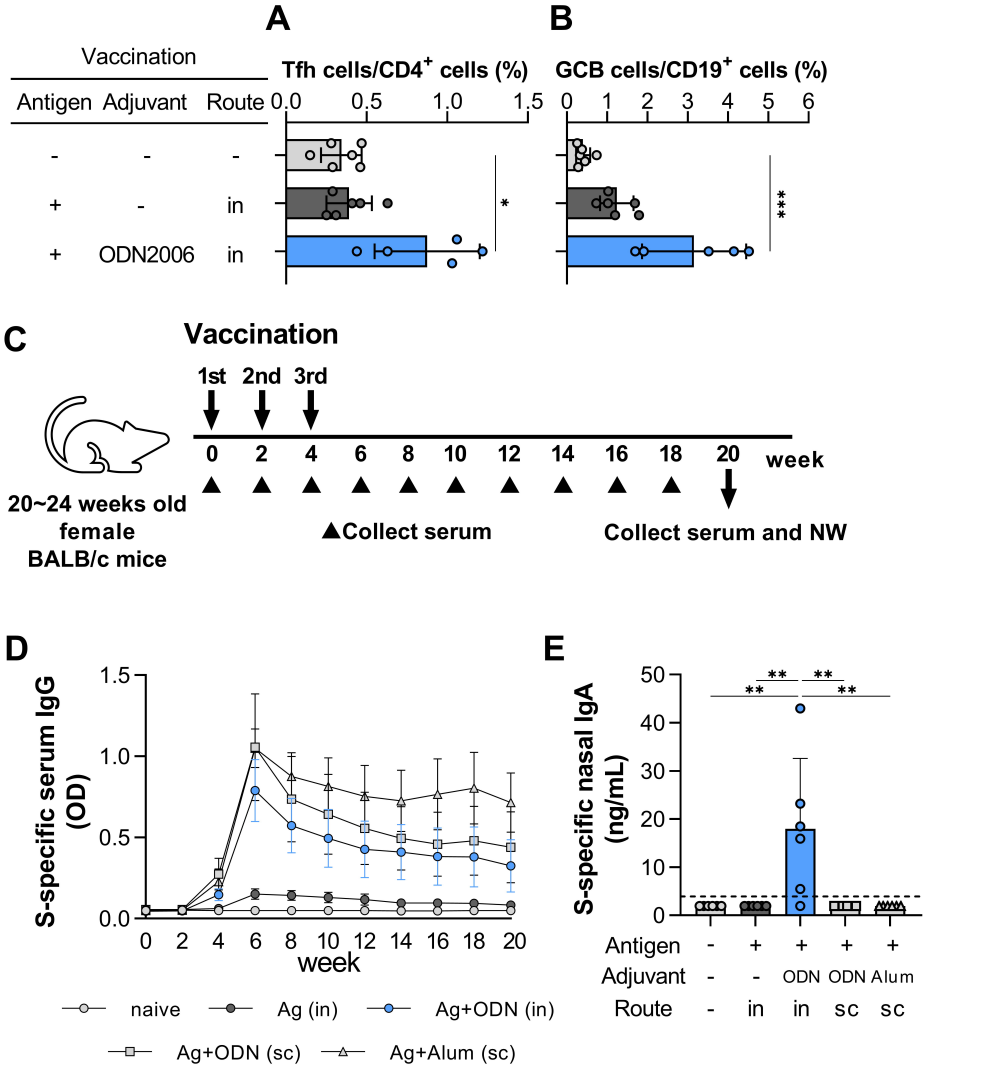
A
B
Vaccination
Antigen Adjuvant Route
- - -
+ - in
+ ODN2006 in
Tfh cells/CD4+ cells (%)
0.0 0.5 1.0 1.5
GCB cells/CD19+ cells (%)
0 1 2 3 4 5 6
*
***
C
Vaccination
1st 2nd 3rd
0 2 4 6 8 10 12 14 16 18 20 week
20~24 weeks old female BALB/c mice
▲Collect serum
Collect serum and NW
D
S-specific serum IgG (OD)
1.5 1.0 0.5 0.0
0 2 4 6 8 10 12 14 16 18 20
week
naive
Ag (in)
Ag+ODN (in)
Ag+ODN (sc)
Ag+Alum (sc)
E
S-specific nasal IgA (ng/mL)
50 40 30 20 10 0
**
**
**
**
Antigen - + + + +
Adjuvant - - ODN ODN Alum
Route - in in sc sc

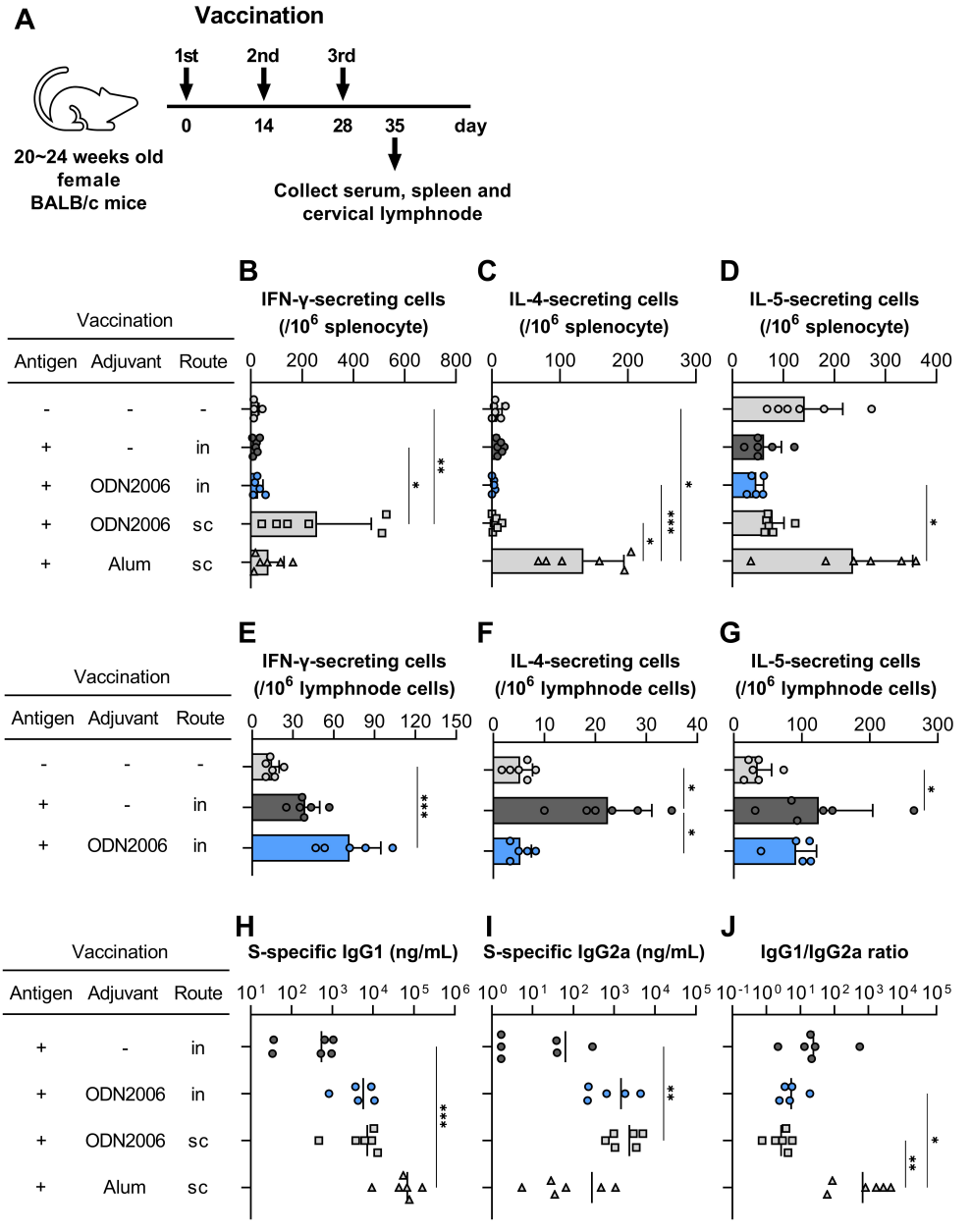
A
Vaccination
1st
2nd
3rd
0
14
28
35
day
20~24 weeks old female BALB/c mice
Collect serum, spleen and cervical lymphnode
B
IFN-γ-secreting cells (/10^6 splenocyte)
C
IL-4-secreting cells (/10^6 splenocyte)
D
IL-5-secreting cells (/10^6 splenocyte)
Vaccination
Antigen Adjuvant Route
- - -
+ - in
+ ODN2006 in
+ ODN2006 sc
+ Alum sc
E
IFN-γ-secreting cells (/10^6 lymphnode cells)
F
IL-4-secreting cells (/10^6 lymphnode cells)
G
IL-5-secreting cells (/10^6 lymphnode cells)
H
S-specific IgG1 (ng/mL)
I
S-specific IgG2a (ng/mL)
J
IgG1/IgG2a ratio

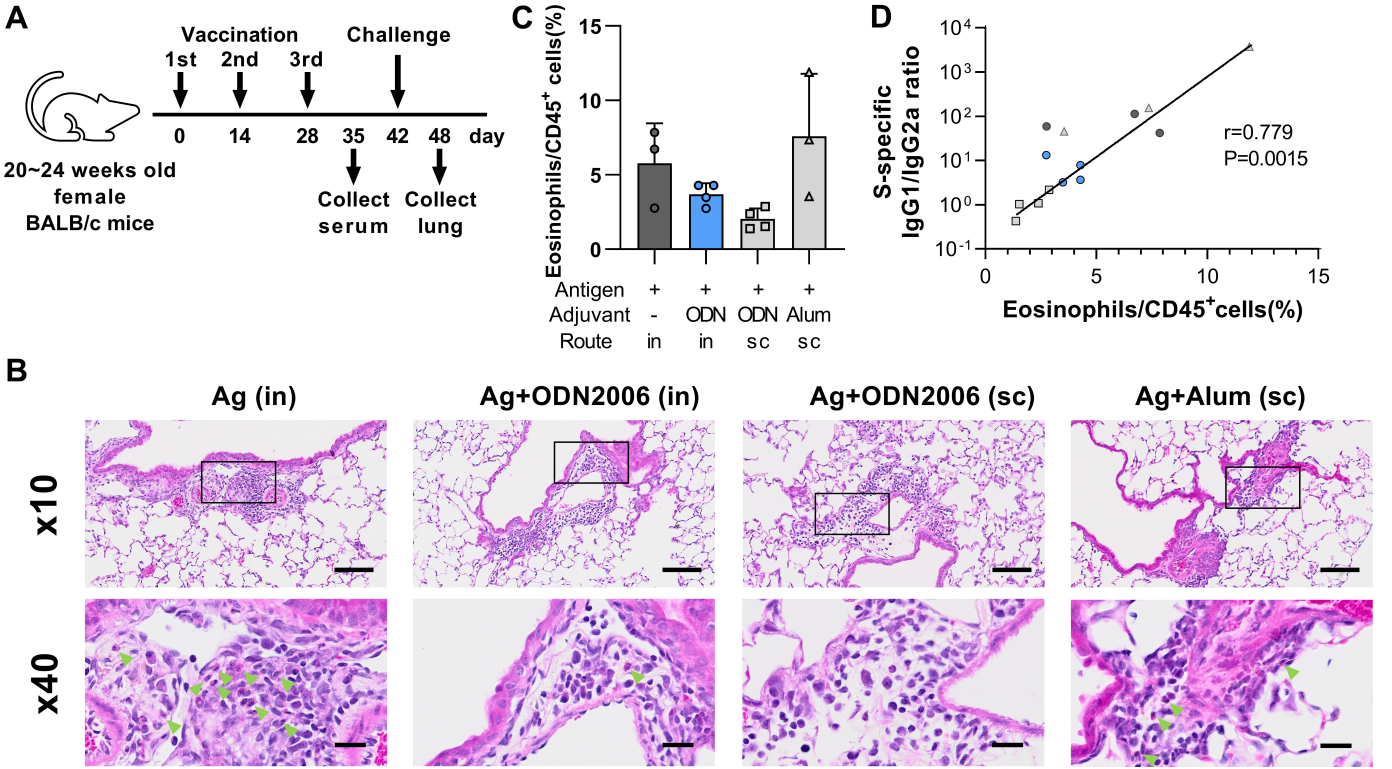
A
Vaccination
Challenge
1st
2nd
3rd
0
14
28
35
42
48
day
20~24 weeks old female BALB/c mice
Collect serum
Collect lung
C
Eosinophils/CD45+ cells(%)
Antigen + + + +
Adjuvant - ODN ODN Alum
Route in in sc sc
D
S-specific IgG1/IgG2a ratio
r=0.779
P=0.0015
Eosinophils/CD45+cells(%)
B
Ag (in)
Ag+ODN2006 (in)
Ag+ODN2006 (sc)
Ag+Alum (sc)
x10
x40